Electronic Supplementary Information for

Self-assembled Fe_3O_4 nanoparticle-doped TiO_2 nanorod superparticles with highly enhanced lithium storage properties

Bin Xue [a, b], Tongtao Li [a], Biwei Wang [a], Li Ji [a], Dong Yang [b], Angang Dong [a,*]

[a] *Collaborative Innovation Center of Chemistry for Energy Materials, Shanghai Key Laboratory of Molecular Catalysis and Innovative Materials, and Department of Chemistry, Fudan University, Shanghai 200433, China.*

[b] *State Key Laboratory of Molecular Engineering of Polymers (Fudan University), Shanghai 200433, China*

*Corresponding author.
E-mail: agdong@fudan.edu.cn (A. D).

The calculation of ratio between Fe_3O_4 and TiO_2 for $Fe_3O_4/(TiO_2)_{70}$.

$m\ (TiO_2) = c\ (TiO_2) \times V\ (TiO_2) = 40\ \text{mg/mL} \times 1.820\ \text{mL} = 72.8\ \text{mg}$

$m'(\text{single } TiO_2\ \text{NR}) = \rho\ (TiO_2) \times V\ (\text{single } TiO_2\ \text{NR})$

$= 3.9\ \text{g/cm}^3 \times \pi \times (5 \times 10^{-7}\ \text{cm})^2 \times 5 \times 10^{-6}\ \text{cm}$

$= 1.53 \times 10^{-17}\ \text{g} = 1.53 \times 10^{-14}\ \text{mg}$

$n\ (TiO_2) = m\ (TiO_2)\ /\ m'(\text{single } TiO_2\ \text{NR})$

$= 72.8\ \text{mg} /1.53 \times 10^{-14}\ \text{mg}$

$= 4.76 \times 10^{15}$

$m\ (Fe_3O_4) = c\ (Fe_3O_4) \times V\ (Fe_3O_4) = 40\ \text{mg/mL} \times 0.182\ \text{mL} = 7.28\ \text{mg}$

$m'(\text{single } Fe_3O_4\ \text{NP}) = \rho\ (Fe_3O_4) \times V\ (\text{single } Fe_3O_4\ \text{NP})$

$= 5.2\ \text{g/cm}^3 \times 4/3 \times \pi \times (1.7 \times 10^{-6}\ \text{cm})^3$

$= 1.07 \times 10^{-16}\ \text{g} = 1.07 \times 10^{-13}\ \text{mg}$

$n\ (Fe_3O_4) = m\ (Fe_3O_4)\ /\ m'(\text{single } Fe_3O_4\ \text{NP})$

$= 7.28\ \text{mg}\ /\ 1.07 \times 10^{-13}\ \text{mg}$

$= 6.80 \times 10^{13}$

$n\ (TiO_2)\ /\ n\ (Fe_3O_4) = 4.76 \times 10^{15}\ /\ 6.80 \times 10^{13} = 70/1$

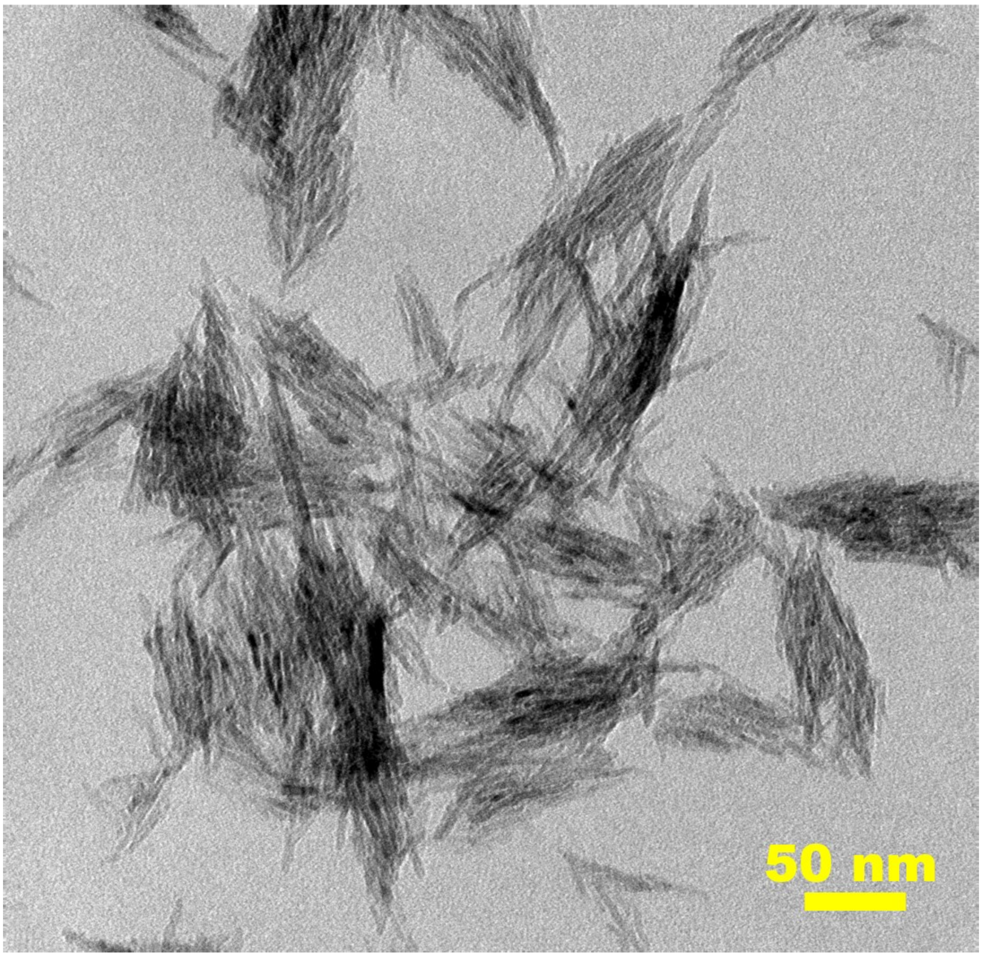

Fig. S1 High-magnification TEM image of TiO_2 NRs.

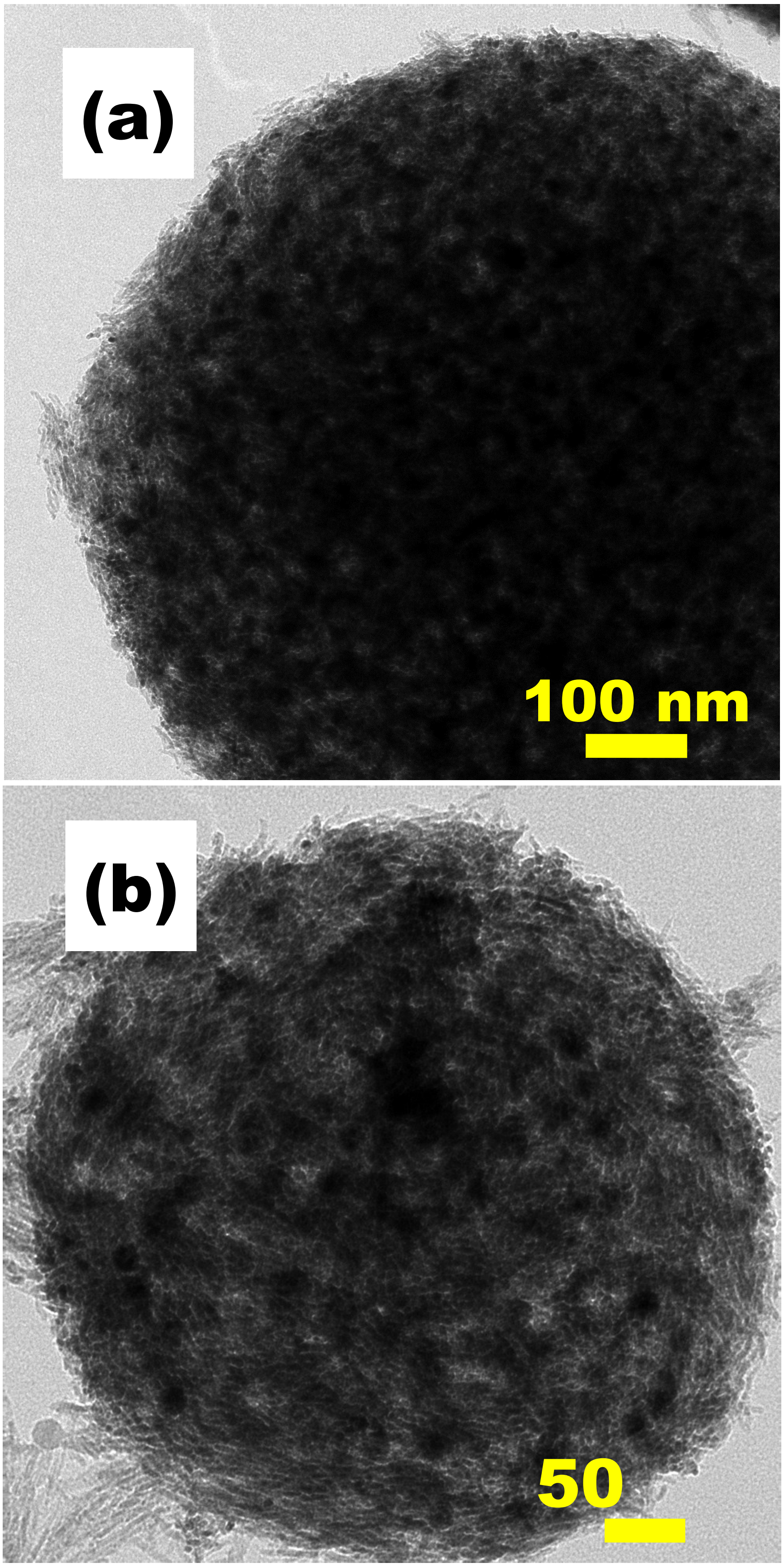

Fig. S2 TEM image of (a) enlarged Fig. 3e and (b) a smaller $Fe_3O_4/(TiO_2)_{70}$ SPs.

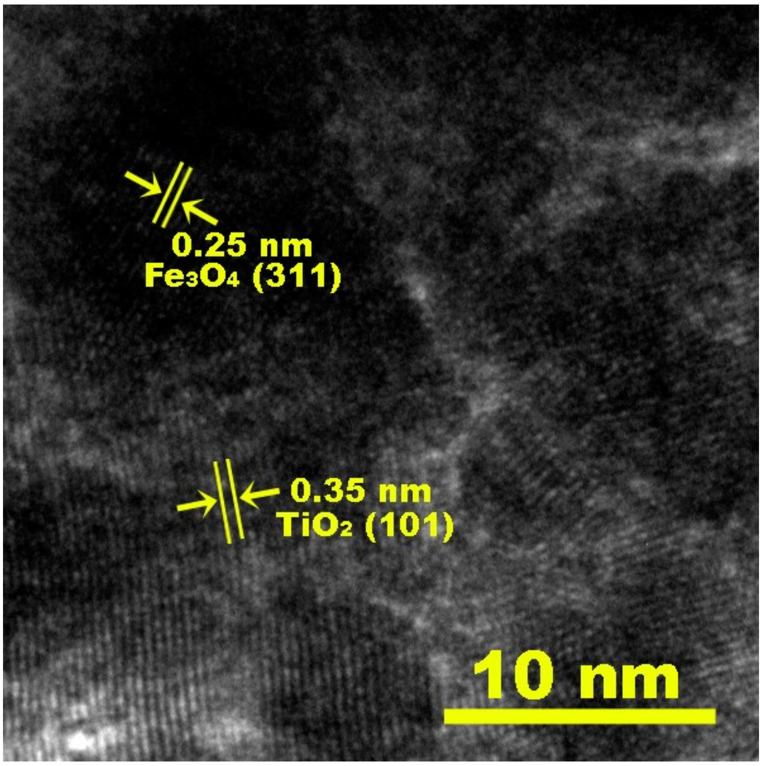

Fig. S3 HRTEM image of $Fe_3O_4/(TiO_2)_{70}$ SPs

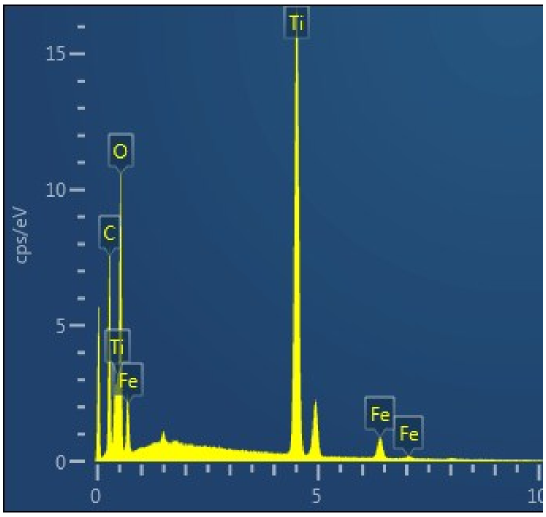

Fig. S4 EDS analysis on the cross-section of the $Fe_3O_4/(TiO_2)_{70}$ SPs after ion-beam cutting.

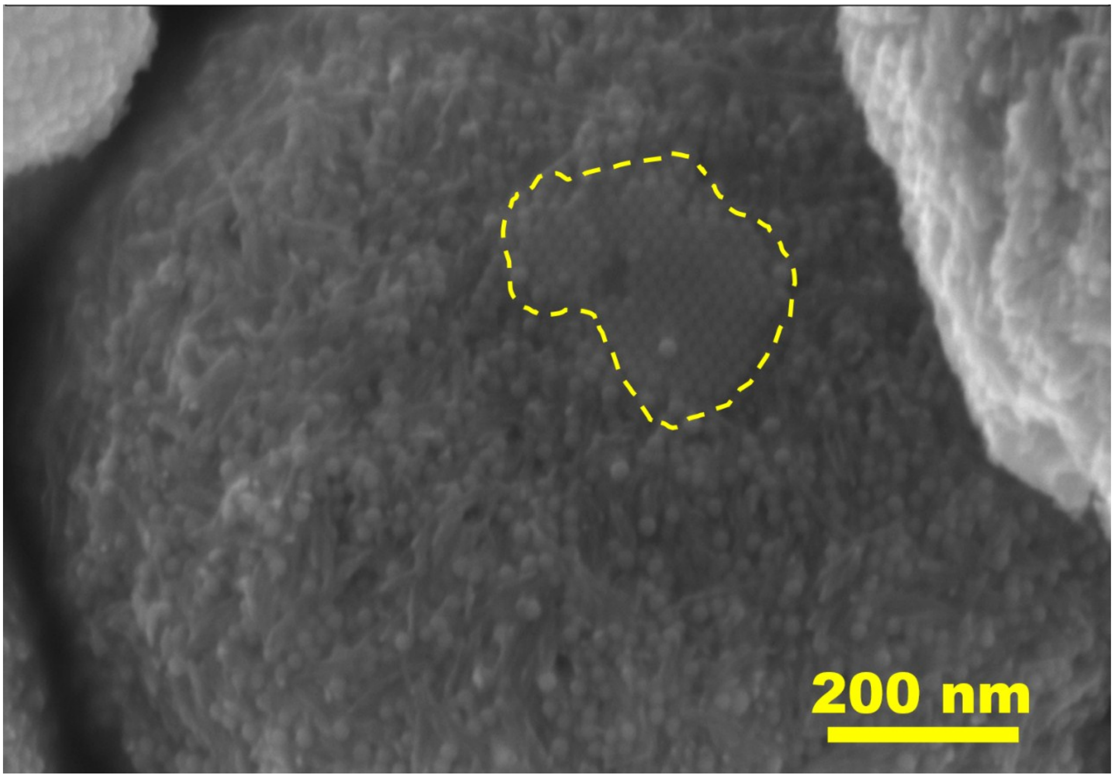

Fig. S5 FESEM image of phase separation in the $Fe_3O_4/(TiO_2)_7$ SPs.

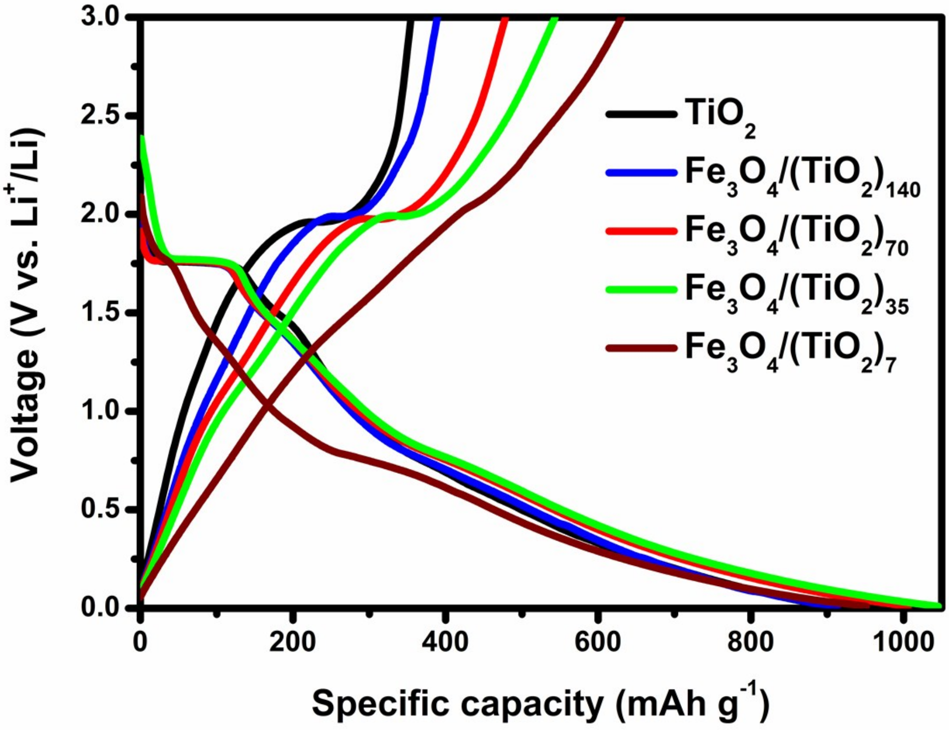

Fig. S6 First galvanostatic charge/discharge curves of the TiO_2 NRs and Fe_3O_4 NP doped-TiO_2 NR SPs at 100 mA g^{-1}.

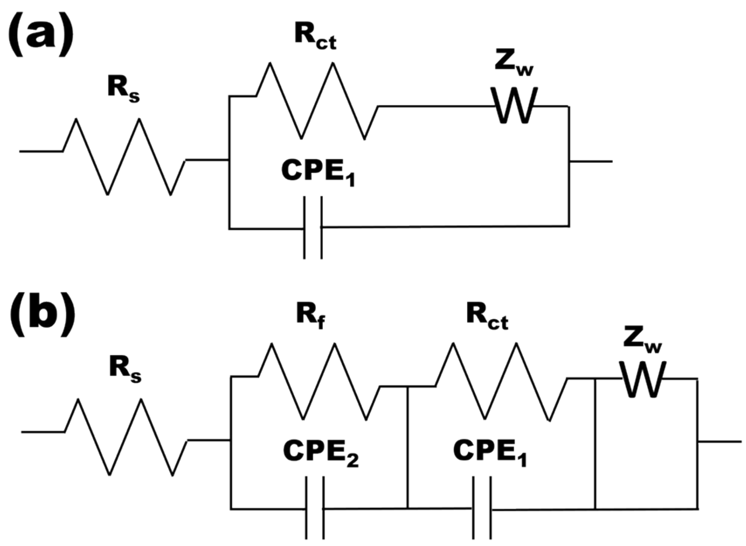

Fig. S7 The equivalent circuit modes for fitting the EIS in (a) Fig. 6e and (b) Fig. 6f. (R_s, ohmic resistance; R_{ct}, charge transfer resistance; CPE_1, interfacial capacitance at the electrode/electrolyte interface; Z_w, Warburg resistance; R_f, surface layer resistance; CPE_2, surface layer capacitance.)

Table S1 Impedance parameters of the fitting equivalent circuit.

Samples		R_s (Ω)	R_f (Ω)	R_{ct} (Ω)
Before cycling	TiO_2 SPs	5.52	-	531
	$Fe_3O_4/(TiO_2)_{70}$	1.18	-	112
After cycling	TiO_2 SPs	1.41	41.3	127
	$Fe_3O_4/(TiO_2)_{70}$	0.869	5.89	32.3

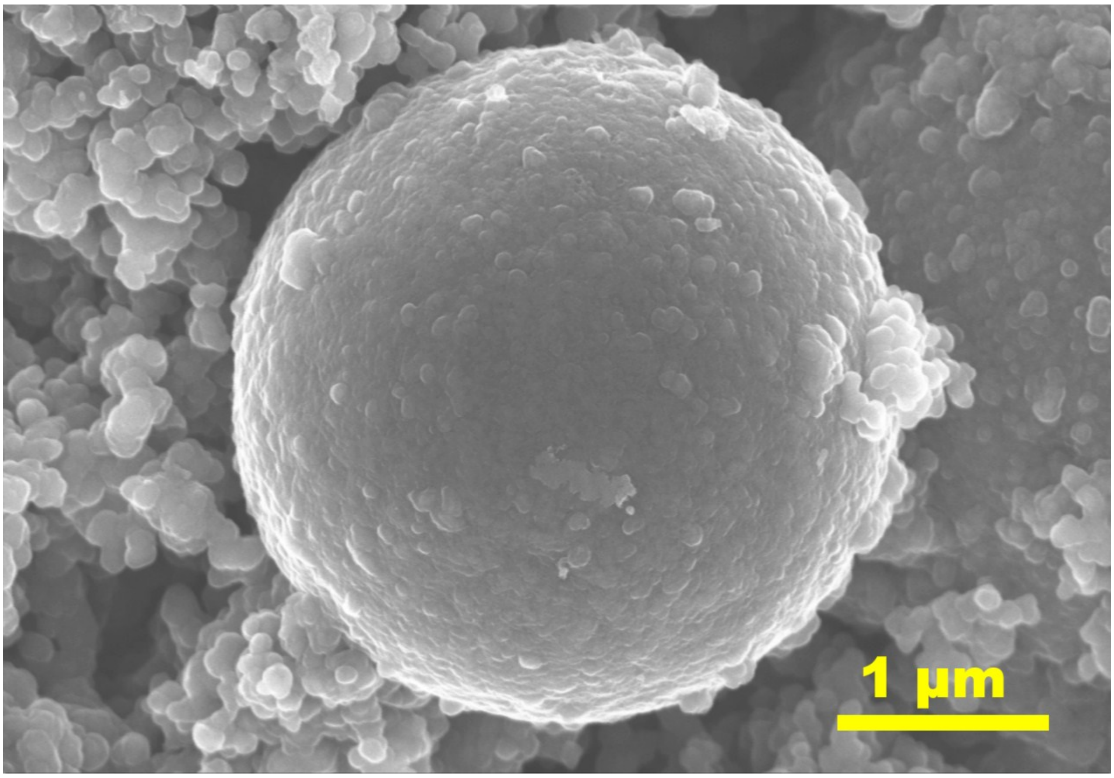

Fig. S8 Enlarged *ex-situ* FESEM image of the $Fe_3O_4/(TiO_2)_{70}$ SPs after cycling.

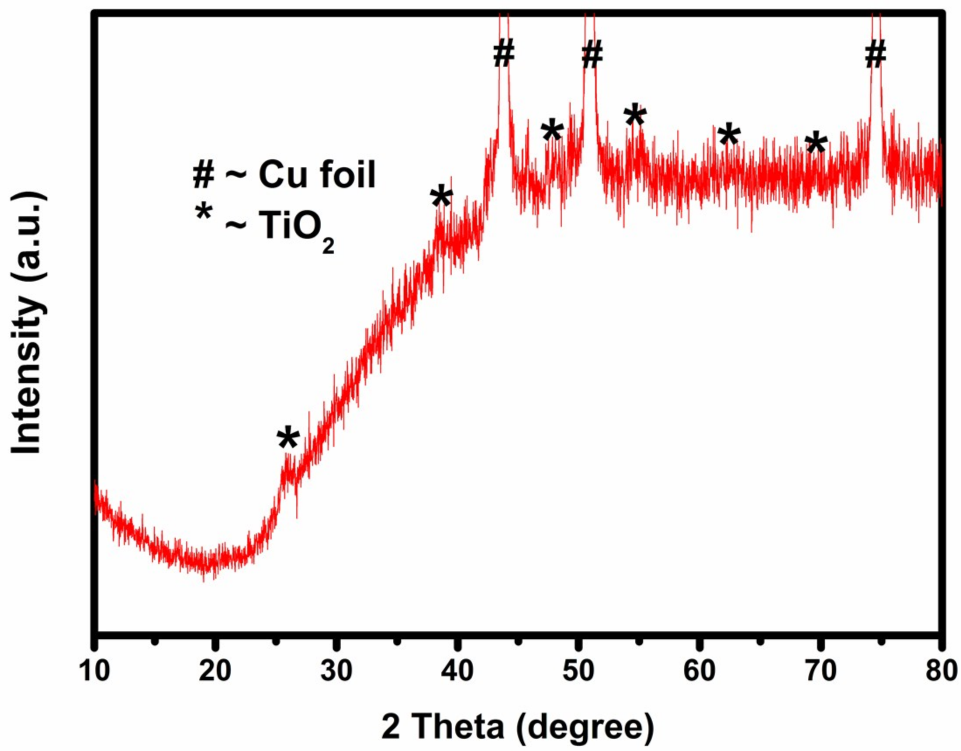

Fig. S9 *Ex-situ* XRD pattern of the $Fe_3O_4/(TiO_2)_{70}$ SPs after cycling.

Table S2 Lithium storage performance comparison between $Fe_3O_4/(TiO_2)_{70}$ SPs and representative TiO_2-based composite anode materials.

Materials	Weight ratio (%)	Capacity (mAh g^{-1})	Cycles	Current density (mA g^{-1})	References
Hierarchical nanofibrous Fe_3O_4-TiO_2-carbons composite	32.5 of Fe_3O_4 content	525	100	100	S1
Carbon-coated TiO_2(B) nanosheets decorated with Fe_3O_4 nanoparticles	TiO_2:Fe_3O_4:C 72.31:19.23:7.99	763	200	500	S2
Fe_3O_4-nanoparticle-decorated TiO_2 nanofiber hierarchical heterostructures	18.2 of iron content	454.5 187.8	200 400	100 1000	S3
Nanoporous TiO_2/Co_3O_4 composite	TiO_2:Co_3O_4 70.5:29.5	290	500	100	S4
ZnO decorated TiO_2 nanosheet composites	TiO_2:ZnO 66.2:33.8	340.2	100	200	S5
Hierarchal mesoporous SnO_2@C@TiO_2 nanochains	73.7 of TiO_2 content	369	100	100	S6
Porous ternary TiO_2/$MnTiO_3$@C hybrid microspheres	TiO_2:$MnTiO_3$:C 75.09:20.18:4.73	402.6	300	100	S7
Lattice-mismatched core-shell TiO_2@MoS_2	TiO_2:MoS_2 25.9:74.1	632	100	100	S8
$Fe_3O_4/(TiO_2)_{70}$ SPs	TiO_2:Fe_3O_4:C 82:7.7:10.3	526 550	100 400	100 1000	This work

References

(S1) Li, S.; Wang, M.; Luo, Y.; Huang, J. Bio-Inspired Hierarchical Nanofibrous Fe_3O_4-TiO_2-Carbon Composite as a High-Performance Anode Material for Lithium-Ion Batteries. *ACS Appl. Mater. Interfaces* **2016**, *8*, 17343-17351.

(S2) Xu, H.; Zhu, X. D.; Sun, K. N.; Liu, Y. T.; Xie, X. M. Elaborately Designed Hierarchical Heterostructures Consisting of Carbon-Coated TiO_2(B) Nanosheets Decorated with Fe_3O_4 Nanoparticles for Remarkable Synergy in High-Rate Lithium Storage. *Adv. Mater. Interfaces* **2015**, *2*, 1500239.

(S3) Wang, H.; Wang, G.; Yuan, S.; Ma, D.; Li, Y.; Zhang, Y. Fe_3O_4-Nanoparticle-Decorated TiO_2 Nanofiber Hierarchical Heterostructures with Improved Lithium-Ion Battery Performance over Wide Temperature Range. *Nano Res.* **2015**, *8*, 1659-1668.

(S4) Zhao, D.; Hao, Q.; Xu, C. Nanoporous TiO_2/Co_3O_4 Composite as an Anode Material for Lithium-Ion Batteries. *Electrochim. Acta* **2016**, *211*, 83-91.

(S5) Gao, L.; Li, S.; Huang, D.; Shen, Y.; Wang, M. ZnO Decorated TiO_2 Nanosheet Composites for Lithium Ion Battery. *Electrochim. Acta* **2015**, *182*, 529-536.

(S6) Luo, G.; Liu, W.; Zeng, S.; Zhang, C.; Yu, X.; Fang, Y.; Sun, L. Hierarchal Mesoporous SnO_2@C@TiO_2 Nanochains for Anode Material of Lithium-Ion Batteries with Excellent Cycling Stability. *Electrochim. Acta* **2015**, *184*, 219-225.

(S7) Guo, S.; Liu, J.; Qiu, S.; Liu, W.; Wang, Y.; Wu, N.; Guo, J.; Guo, Z. Porous Ternary TiO $_2$/$MnTiO_3$@C Hybrid Microspheres as Anode Materials with Enhanced Electrochemical Performances. *J. Mater. Chem. A* **2015**, *3*, 23895-23904.

(S8) Dai, R.; Zhang, A.; Pan, Z.; Al-Enizi, A. M.; Elzatahry, A. A. Hu, L.; Zheng, G. Epitaxial

Growth of Lattice-Mismatched Core-Shell TiO_2@MoS_2 for Enhanced Lithium-Ion Storage. *Small* **2016**, *12*, 2792-2799.